IEEE Access
Multidisciplinary | Rapid Review | Open Access Journal

Received January 20, 2022, accepted March 8, 2022, date of publication April 5, 2022, date of current version April 14, 2022.

Digital Object Identifier 10.1109/ACCESS.2022.3165023

Optimizing Daylight Glare and Circadian Entrainment in a Daylight-Artificial Light Integrated Scheme

VEENA MATHEW[1], (Member, IEEE), CIJI PEARL KURIAN[1], (Senior Member, IEEE), AND NEVIN AUGUSTINE[2]

[1]Department of Electrical and Electronics Engineering, Manipal Institute of Technology, Manipal Academy of Higher Education, Manipal 576104, India
[2]Department of Instrumentation and Control Engineering, Manipal Institute of Technology, Manipal Academy of Higher Education, Manipal 576104, India

Corresponding author: Ciji Pearl Kurian (ciji.pearl@manipal.edu)

This work was supported by the All India Council for Technical Education (AICTE) through the Research Promotional Scheme (RPS) India Funded Project under Grant 8-T4/FDC/RPS (Policy-l) /2019–2020.

ABSTRACT Human circadian rhythm varies with different combinations of light sources. Natural light and dark patterns regulate the sleeping and waking cycles of the human body. This study aimed to develop a simplified model for daylight glare and circadian entrainment in an existing controlled daylight-artificial light integrated system. In addition, the effects of window orientation, occupant position, artificial light, daylight, and a combination of both on Circadian Stimulus (CS) were investigated. In a daylit interior space, window orientation, shading control and occupant seating position play a significant role in the CS. Simplified models to predict Daylight Glare Probability (DGP) and CS were estimated from the dataset. The developed nonlinear CS estimation models have R-squared values of 0.983 and 0.974. The precision of the models was evaluated in terms of standard error of regression (S) and AIC score. Multi-Objective Genetic Algorithm based optimization technique was developed using the above models to minimize glare and maximize CS in the working space. This optimisation methodology aids in implementing a complete automation algorithm for the test workbench to achieve visual comfort and circadian entrainment.

INDEX TERMS Circadian stimulus, vertical eye illuminance, daylight glare probability, non-linear regression models, multi-objective genetic algorithm optimization.

I. INTRODUCTION

The biological clock of humans is directly correlated with natural light and dark patterns [1]–[3]. It also regulates the sleeping and waking cycle of the human body. Various light exposures can alter the responses of the circadian system and these effects can be predicted using different mathematical models [4]–[6]. In contrast to the visual system, the circadian system begins at the retina and moves toward the suprachiasmatic nuclei (SCN) located in the hypothalamus of the brain. The other vital parts of the circadian system include the retinal hypothalamic tract (RHT) and pineal gland. The system follows the RHT path and advances toward the paraventricular nucleus (PVN) and superior cervical ganglion to the pineal gland. At night, reduced lighting condition helps in the secretion of melatonin hormone in the pineal gland and circulates throughout the body [7]. Recently discovered melanopsin photoreceptors, also called intrinsically photosensitive retinal ganglion cells (ipRGC), paved the way for various cone and melanopic sensitivity functions [6], [8]. Owing to the intervention of artificial light, various shading devices, other architectural and climatic features in closed spaces, the synchronization of the human circadian system result in lead or lag. Disruption of the natural circadian rhythm eventually leads to reduced alertness, mood variations and sleep pattern changes [9]–[15].

Similar to CIE Standard Observer response curve V(λ), researchers put forward different mathematical functions to evaluate the circadian light [4], [16]–[19]. Different metrics are in the developmental stage to assess the circadian impact on an occupant. Various standards, regulations and recommended actions are put forward in the world lighting

The associate editor coordinating the review of this manuscript and approving it for publication was Santosh Kumar.

community to enhance the non-visual activities of the occupants [20]–[25]. Based on the spectral power distribution and the α-opic illuminance, lighting researchers initiated the quantification of non-visual effects [5]. The α-opic illuminances aided to interpret a quantity for each of the five known photopigments in the eye. These quantities are evaluated by weighting the incident light on the corneal level with the individual spectral sensitivity functions of the photopigments with the eye lens transmission of a 32-year-old Standard Observer. Later utilizing the spectral sensitivity functions, the national standards committee ''Deutsches Institut für Normung'' (DIN) established melanopic factor of luminous radiation $a_{mel,}$ and melanopic daylight equivalent illuminance $E_{v,mel,D65}$. These metrics represent the effect of light on a single photopigment called melanopsin. But the circadian system's sensitivity also depends on the signals from other photoreceptors, i.e., cones and rods. Parallel to this, the ''International WELL Building Institute'' (IWBI) put forward melanopic ratio $R_{mel,\ ratio}$ and equivalent melanopic lux EML [20]–[22], which are based on the melanopsin sensitivity function. In 2018, the International Commission on Illumination CIE published its metric system for quantifying the impact of incident light on photoreceptors [23]. CIE system followed the previous approach of the α-opic illuminance and calculated the quantities for each photoreceptor where the difference appears only in the normalization of the quantities.

All these metrics are beneficial in revealing the effect of each photoreceptor channel on an output parameter. But they did not consider the complicated neuroanatomy of the retina and the signal passages in the brain. The non-visual effect of light on melatonin suppression or human circadian rhythm cannot be described by a quantity established on a single photopigment. In contrast to the above metrics, the Lighting Research Institute (LRC) developed a new metric called Circadian Stimulus (CS), which incorporates complex neuroanatomy, neurophysiology, and the circadian system's characteristics. This metric underwent yearly revisions, and the latest revised metric called Circadian Stimulus (CS_{2018}) increased its accuracy by explaining the melatonin suppression and human circadian system [4], [11], [24], [25]. Neurophysiology plays a vital role in incorporating other visual effects like brightness, visual clarity, scene preference and colour preference.

Recommendations regarding CS for academic and office purposes have been defined and applied in various field studies[12], [13], [26]–[28]. CS varies from 0 to saturation of 0.7. A minimum of CS 0.3 is recommended for circadian entrainment at least for two continuous hours during the daytime. The average CS can be calculated as shown in (1). Circadian Light (CL_A) is spectrally weighted irradiance of the human circadian system.

$$\boldsymbol{CS = 0.7 * \left(1 - \frac{1}{1 + \left(\frac{CL_A}{355.7}\right)^{1.1026}}\right)} \tag{1}$$

CS represents the effectiveness of CL_A or the amount of nocturnal melatonin suppression after an hour of light exposure [4], [11]. For example, a CS of 0.3 indicates that 30% of nocturnal melatonin secretion is suppressed, assuming the diameter of the eye pupil is 2.3 mm. Hence as CS moves toward saturation, more hormonal suppression occurs. As previously discussed, to suppress the melatonin hormone secreted by pineal gland, light passes through the SCN, the primary pacemaker of the human biological clock. Thus, light stimulates the circadian clock via SCN. This indicates the indirect effect of CS thresholds on sleep quality and well-being in humans.

Daylight is a perfect light source for synchronization of human circadian system [29], [30]. Various studies have also established the impact of vertical eye illuminance and Correlated Colour Temperature (CCT) on circadian entrainment [29]–[39]. It is suggested that to optimize interior light availability to meet the circadian criteria of the occupants, these factors need to be considered. An interior daylit space can be controlled either by manual control or a closed-loop control scheme [33], [40], [41]. The user preference model can be easily incorporated by fixing the setpoints according to the preference [42]. Daylight fused with tunable LEDs in human-centric lighting enhances occupant performance by improving visual comfort and mood behaviour [42]–[44]. Enhancing the effectiveness of daylight augments the non-visual response of humans to light.

While automating a daylit interior space, designers mainly focus on maximum visual comfort with significantly less glare. Artificial light should supplement the natural sunlight without compormising the occupant's eye level comfort. Glare is the primary dimension of visual comfort in a room. This indicates excessive luminance or contrast in a field of view [45], [46]. The main subdivisions of glare are discomfort and disability. The discomfort glare based on subjective responses can be quantified with various glare metrics [47]. Daylight glare metrics are defined based on the luminance of the glare source, the size of the glare source, position index and scene luminance [48]–[50]. Daylight Glare Index (DGI), CIE Glare Index (CGI), Visual Comfort Probability (VCP), Unified Glare Rating (UGR) and Daylight Glare Probability (DGP) are widely used daylight glare metrics in lighting simulations [45], [46].

Recently, the Daylight – Artificial light integration system (DALIS) [51]–[55] has received significant attention. With advancements in technology, various artificial lighting control schemes have been developed to reduce energy consumption by optimum usage of luminaires in the presence of daylight [44], [56]. As a result, over the last 25 years, the global lighting market has undergone enormous growth. These systems incorporate shading, blinds, switchable films or dynamic glazing, which are controlled in adaption to Daylight [57]–[61]. The robust control of shading devices and luminaires without losing the dynamic nature of a DALIS system is the biggest challenge for lighting designers and it plays a significant role in the evolution of automated blinds

in daylit spaces. In 1996, fuzzy logic algorithms for Venetian Blind controls were developed [62], [63]. Improved versioned projects such as the real-time operation DELTA in 1996 and NEUROBAT in 1998 are pioneers.

II. MATERIALS AND METHODS

As previously mentioned, the computation of CS requires costly spectrometers or daysimeters [64]. This requires a large amount of investment to carry out experimentation. Therefore, the first objective is to mathematically compute the CS with generally known photometric quantities that are easily measurable. Owing to the inherent non-linearity in CS as in equation (1), the model estimation was performed using the non-linear regression method. Here the model function shown in equation (1). Vertical eye illuminance (E_v) and CCT were selected as independent variables for model evaluation.

Generally, any class of functions can be evaluated using non-linear least squares estimation [65]. Unlike linear regression, the limitations are very small when using the parameters in non-linear regression. Non-linear regression techniques use measured data to form a model with non-linear functions and one or more independent variables. The efficient use of data provides reasonable estimates of unknown parameters. Successive approximations were used to implement data fitting. Once the model was developed, its performance was evaluated using residual plots, Error of Sum Squares (SSE), Coefficient of determination (R square-R^2), Root Mean Squared Error (RMSE), and Adjusted R-square[66].

The next goal of this work is to investigate glare issues and how they can be incorporated into CS. Various studies have shown the relevance of E_v over other complex glare metrics (such as DGI, UGR, and CGI) in predicting glare sensation [67]. Another metric called [68] the 'Daylight Glare Probability (DGP), indicates the per cent of occupants disturbed by a daylighting glare scene. The glare sensation is rated using the equation (2):

$$DGP = 5.87 \times 10^{-5} E_V + 9.18 \times 10^{-12} \times log\left(1 + \sum_i \frac{L_{s,i}^2 w_{s,i}}{E_v^{1.87} P_i^2}\right) + 0.16 \quad (2)$$

where E_v is the vertical eye illuminance (lux); L_{si} is the luminance of the i^{th} light source in the visual scene (Cd/m^2), ω_{si} is the solid angle of the i^{th} scene light source (sr) and P is the Guth position index.

The DGP was implemented in Radiance through Evalglare, a tool used to evaluate various glare metrics. Using an HDR image, Evalglare estimated the daylight glare on an annual basis perceived at a point [69]. The performance and reliability of numerous established glare metrics were compared through measurements conducted out in office-like test rooms located in six different locations [70]. The researchers found that the DGP is more reliable for discriminating between disturbing and non-disturbing. In addition, the metrics that account for the saturation effect in their equation, such as DGP, $PGSV_{saturated}$ and UGR_{exp}, perform better in daylight-dominated workplaces than purely empirical metrics.

Recently, many studies have proposed methods to calculate DGP in a fast and accurate manner. By omitting the contrast term, a simplified linear regression model solely on E_v was developed by the authors as shown in equation (3):

$$DGP = 0.184 + 6.22 \times 10^{-5} E_v \quad (3)$$

However, this model is applicable in scenes where ''no direct sun or a specular reflection of it hits the eye of the observer'' [71].

The test room located at MIT-Manipal is designed to perform various simulations and performance analyses of the automation algorithms for daylight-electrical light integration. The fuzzy logic algorithm in the LabVIEW platform is implemented on an industry-standard myRIO controller (National Instruments). The climate-responsive operation of Venetian Blind and the controller integrated with the test room provides real-time performance analysis. The test room is automated for energy optimization and maximum visual and thermal comfort [51]–[53]. The control algorithms successfully captured the dynamic nature of our DALIS system. However, the main limitation of this system is that it does not incorporate the need for circadian stimulation of the occupants. This system optimizes energy consumption, visual comfort, and thermal comfort, but not CS. The final objective was to derive an optimum solution set of photometric quantities directly linked to the occupant's circadian entrainment and visual comfort. Hence the above- derived models of CS and DGP can further be optimized to achieve this goal. The primary considerations of this optimization are to minimize glare and maximize CS.

This optimization problem was solved using an evolutionary optimization algorithm called Multi-Objective Genetic Algorithms (MOGA)[72]. In this optimization problem, a controlled elitist genetic algorithm (CEGA), which is an adaptation of the non-dominated sorting genetic algorithm II (NSGA-II)[73], is used. Elitism prevents evolutionary algorithm without losing the set of reasonable solutions. The simulations were performed in the GA toolbox using the MATLAB platform. NSGA-II is an elitist mechanism that provides a packed comparison operator with a relatively low computational complexity. In addition, it shows more convergence compared to the original NSGA-II.

The experiments were conducted in a controlled daylight-artificial light integrated room consisting of an automated Venetian Blind and daylight adaptive dimmable LED luminaires [51]–[53], [74]–[77]. The system maintains interior illuminance, temperature, uniformity, visual comfort (glare), and thermal comfort. The pyranometer, which is kept on top of the building, constantly logs irradiance data into the data logger. The control inputs to the blind system were external daylight on the window, solar altitude, and temperature difference between the setpoint and exterior temperature.

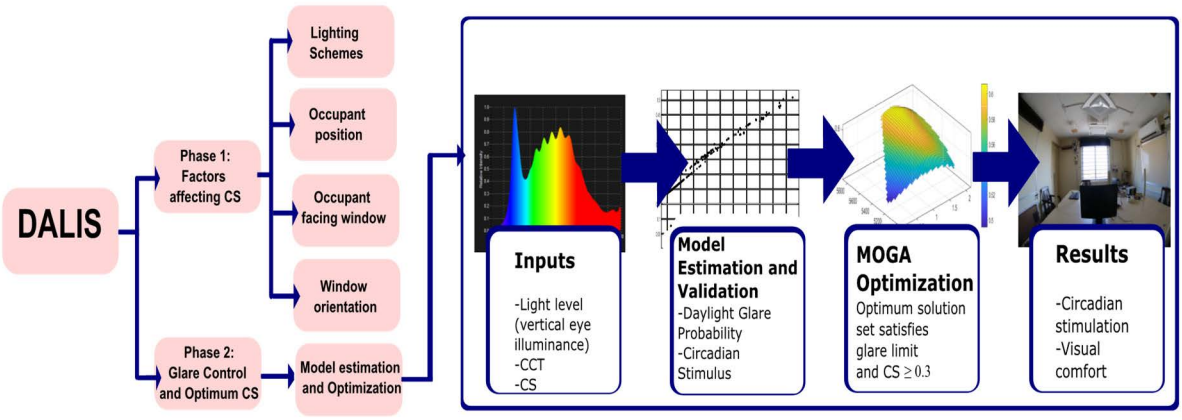

FIGURE 1. Graphical abstract of the work.

This fuzzy-based window blind control system maintains visual and thermal comfort for the occupants and incorporates energy optimization when the occupant is absent. The control system automatically senses the occupancy, and the luminaires turn off/50% dimmed according to the settings.

First, the CS level in the test room was measured under various lighting conditions and the various related factors. Various lighting scenarios include only artificial light, daylight, and controlled daylight - artificial light integrated scheme (DALIS) conditions. As per literature, a minimum threshold of CS $>$ 0.3 for at least 2 h in the daytime provides circadian stimulation to day-active occupants. Previous studies regarding the non-visual effect of light based on the above threshold condition of CS have proven the improvement in the well-being, alertness, and sleep quality of occupants [12], [37]–[39]. Therefore hypothetically, the meeting criteria of this work, that is, CS$>=$0.3, always aids in the circadian entrainment of the occupant. Second, a regression model of CS was obtained from the datasets of various CCT and E_v values. Later, a simplified regression model for DGP with E_v as the single predictor was estimated using the glare dataset derived from Evalglare software. This data set (image) was collected during the experimental verification of the performance of DALIS control schemes. Finally, a multi-objective genetic optimization technique was designed to obtain optimal E_v satisfying glare conditions and CS. The sections detail the experimental setup and room details, modelling, optimizing glare and CS at the observer's eye level, and inferring the data. The primary goals of this study are as follows:

- Explore the effect of window orientation, occupant position, lighting schemes with daylight, artificial light, the combination of both and controlled lighting environment to meet the threshold of CS$\geq$0.3.
- Obtain computation models to evaluate CS without any spectrometers and to predict DGP in the test workbench.
- Finally, incorporate the mathematical models of CS and DGP to optimize the workbench for minimum glare and maximum CS.

Fig.1 shows the graphical abstract of the research work.

A. EXPERIMENTAL INVESTIGATIONS

Experimental investigations were carried out in a test room at MIT-Manipal (13.3525° N, 74.7928° E), a climate-responsive automated control facility for Venetian Blinds and luminaires [51]. The air-conditioned test room has a dimension of 4 m $\times$ 4 m $\times$ 2.3 m with clear glass windows of size 1.3 m $\times$ 1.3 m on all four wall sides, which can be operated one at a time or multiple windows. The binds and luminaire were automated using a climate model-based algorithm implemented on an embedded control platform using LabVIEW. The system is designed to adjust the blind position to achieve visual and thermal comfort and energy saving by maintaining the room temperature and interior illuminance at the given setpoints. The work plane of the room (2m $\times$ 2m) had two zones. The first zone was considered as one window head height from each window, and the second zone was away from the window. The authors developed fuzzy-based [51] and predictive models [74] to predict the blind position to achieve visual comfort, thermal comfort, and energy-savings.

The performance of the automated system was validated by examining the real-time daylight on the window and both zones of the work plane by varying the blind positions from 0% to 100%. Here, the system's predictors are the irradiance input from the pyranometer, temperature input from the sensor and solar altitude.

The position of the window blind (alpha) was obtained as the output data from the fuzzy model, as shown in Fig.2 [51]. Fig. 3 shows the entire system with motor- controlled Venetian blinds and two dimmable LED luminaires. In this work, the investigations were done with different lighting scenarios. The different cases are as follows:

- Only Daylight (DL), i.e., blinds open.
- Only artificial light (AL), i.e., blinds closed.

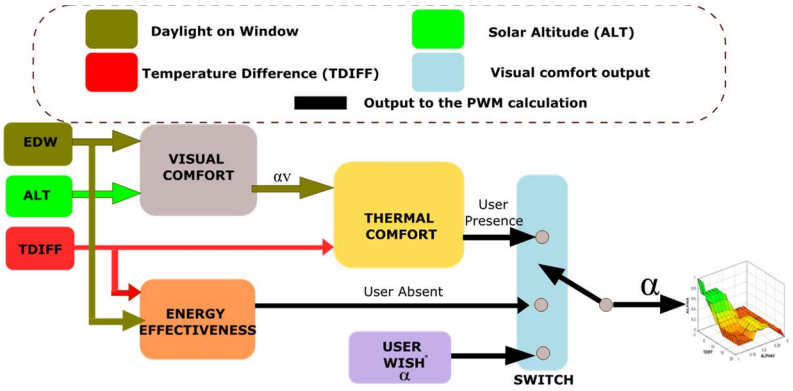

FIGURE 2. Window Blind controller block diagram and visual & thermal comfort 3D surf plot.

FIGURE 3. Interior view of the test room.

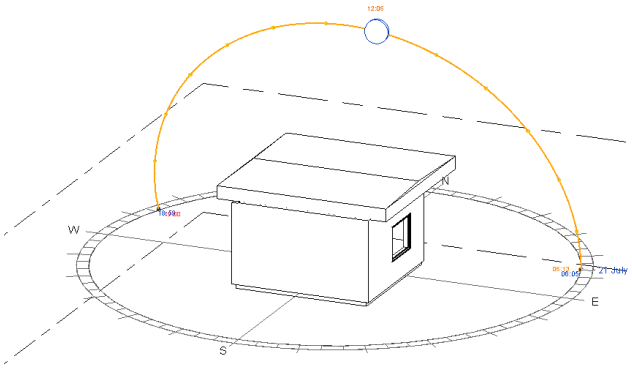

FIGURE 4. Solar path on 21th July at Manipal.

- Daylight and artificial light (DAL), i.e., not controlled, blinds open.
- Daylight and artificial light integrated system (DALIS), controlled.

Here, three weeks of readings during office timings from10 am to 5 pm under clear sky conditions were considered. The solar path on 21st July at Manipal is shown in fig. 4. Eye level/vertical illuminance (Ev), horizontal work plane illuminance (Eh), CCT and spectrum of the light falling at the eye were measured for all orientations. In offices, people do not prefer to see in the window direction to avoid at glare sensation.

Hence, the position of the occupant changed in all sets of measurements. For the same experimental setup, the occupant sat on all four sides of the workplane. This incorporates variations in the vertical plane measurements in all directions. The floor plan of the test room is illustrated in Fig. 5. The illuminance, CCT and spectrum were measured by using a CL-500A spectrophotometer. Circadian metric CS was evaluated using the excel-based LRC toolbox [25]. The horizontal work plane was considered at a height of 0.8 m from the floor level, and vertical illuminance was measured at the eye level height (1.2 m), as shown in Fig. 6. The potential of circadian light is defined as a minimum of 0.3 CS at the occupant's eye level during daytime for at least two hours.

III. RESULTS

Table 1 shows the correlation of CCT and E_v with CS, for which readings were taken in all four orientations with blinds completely open and artificial lights off. A correlation test was done for 1700 samples, to examine the effects of variations in E_v and CCT on changes in CS. The non-linear correlation between the two variables was identified using Spearman's correlation test. Rather than the Pearson's coefficient, which is mostly suitable for obtaining linear correlation the former is more suitable for non linear correlation. Rather than CCT changes, the variation in E_v was highly correlated with the CS.

A. WINDOW ORIENTATION AND OBSERVER FACING TOWARDS THE WINDOW

A window plays a significant role in allowing daylight inside a building. It is well known that proper window design helps in energy savings, visual comfort and thermal comfort [59], [78]–[80]. Different shading controls also help correlate daylight availability with visual comfort in the interior space [56], [60], [81]. Recent studies have demonstrated

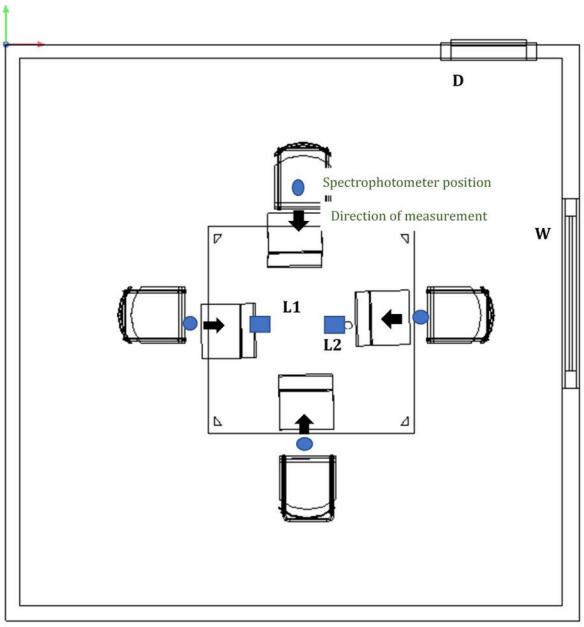

FIGURE 5. Floor plan of the test room including luminaires (L1, L2), window (W), Door (D), Worktable, Laptops, Spectrophotometer position, measurement direction.

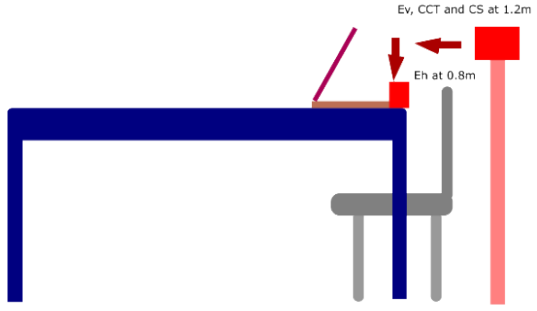

FIGURE 6. Graphical view of the measurement setup.

TABLE 1. Correlation of CCT and E_v with CS.

Spearman's rho Correlation		E_v	CCT
CS	Correlation Coefficient	.898**	.282**
	Sign. (2-tailed)	.000	.000

**. Correlation is significant at the 0.01 level (2-tailed).

an association between daylight and health outcomes [9], [28], [29], [39], [42], [82]. This experiment set was performed to determine the effect of facing an open window at the level of CS. In all cases, the E_v/E_h ratio was higher than 0.8, and CCT was recorded more than 4900 K, as shown in Fig. 7. An occupant facing an open window in any direction during the morning satisfies a CS of 0.3 and above. This situation arises because of the short wavelength in the daylight spectrum which directly falls on the eye.

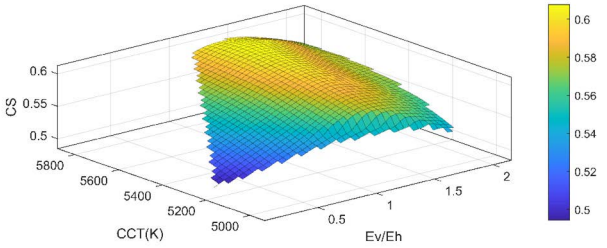

FIGURE 7. Variation in CS with CCT and E_v/E_h while facing an opened window.

A person can occupy a position such that they may face the opened window. However, direct exposure to short wavelength leads to glare issues for the occupants [83]. Therefore, the selection of the seating position is such that there is minimum glare and maximum CS. Thus, a controlled environment reduces the glare problems.

B. OCCUPANT POSITION AND LIGHTING SCHEME

Daylight energises a person's circadian. Receiving daylight with a shorter wavelength at the retina stimulates the alertness and mood of a person. However, it is also essential to control the daylight to eliminate visual discomfort [40], [42], [47], [76]. Hence, it is crucial to determine where a person should occupy the space in a room. Here, the seating position of the occupant was changed to observe the alterations in the CS. In this dataset, the east-oriented window was set to be in the operating condition. The occupant's facing direction was changed to obtain the relevance of seating in the test room. The suitability of the different lighting schemes in the test room was also evaluated based on E_v, E_v/E_h, CS, and CCT. Data were recorded on the same day, at the exact time point. As mentioned in the previous section, each case of the lighting schemes is as follows:- AL-1, DL-2, DAL-3, and DALIS-4. Different colour shading shows the occupant's seating position (sitting in the south, west, north or east) toward the monitor (fig. 8).

Here, the occupant on the west side receives the highest CS than in all lighting schemes and is because the occupant is facing the open east-oriented window, and consequently, more light reaches the eye.

However, this position is not preferred to be occupied in a workspace because of the glare sensation. In comparison with other seating positions, northside provides the minimum CS for circadian entrainment. The DAL scheme provides the highest E_v and, consequently, a high CS among all lighting schemes. However, the E_v/E_h was 37.5% lower than that of the DL scheme. Hence, this indicates the presence of more E_h in the DAL scheme. Compared to the DL scheme, there was a 50% increase in E_h in the DAL owing to artificial light. In the DAL mode, a higher E_v may lead to uncomfortable glare conditions. In the DALIS mode, except for the east side, all other sides were suitable for working with minor settings dimming for a minimum CS value of 0.3. Under these lighting conditions, the Ev/Eh ratio was almost similar

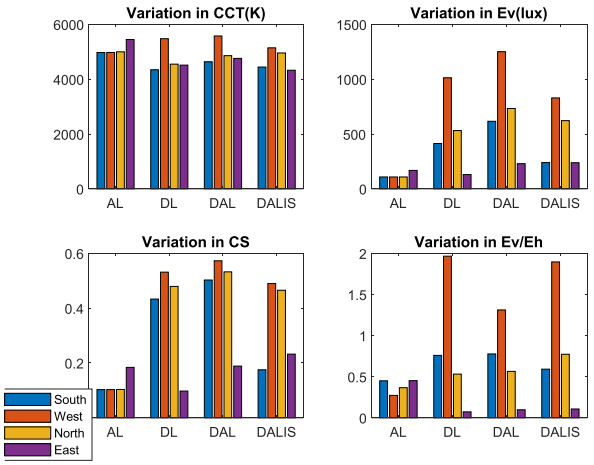

FIGURE 8. Variation in CCT, E_v, CS and E_v/E_h under different lighting schemes.

to that of the DL scheme, but Ev was 25% less. Hence, in terms of CS and glare, the integrated scheme of daylight and electrical light provides a better workspace than other lighting conditions. Fig. 9 shows the variation in CS with CCT and E_v/E_h ratio changes. The maximum observed CS is 0.58. When the E_v/E_h ratio is more than 1, the probability of a CS greater than 0.3 increases. However, a higher Ev/Eh ratio may result in either low E_v and E_h or higher horizontal and vertical illuminance, creating visual discomfort.

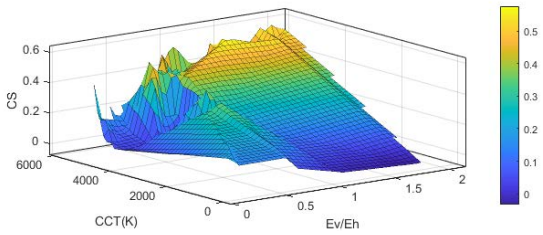

FIGURE 9. Variation in CS with CCT and Ev/Eh.

According to the IESNA lighting standards, the work plane illuminance in a daylit office ranges from 300 lx (intensive computer tasks) to 500 lx (variety of tasks) [84]. These standards help optimize E_v/E_h ratio in interiors to improve visual acuity. Once the horizontal illuminance is set, it becomes easier to derive the proper E_v/E_h ratio.

C. ESTIMATION OF A SIMPLIFIED MODEL FOR GLARE PREDICTION

The dataset for deriving the model for E_v with DGP was obtained from the DALIS controlled room. The daylight glare metric can be obtained using High Dynamic Range (HDR) photographs of daylight scenes and a specific software called Evalglare [68], [70], [85]. Evalglare is radiance-based software that detects glare sources in a 180° HDR fisheye image [56], [86]. Using Evalglare software, the daylight glare was estimated from the HDR images of the scenes. A Canon 750D digital camera, mounted on a tripod, was used to capture HDR images at a height of 1.2m above the floor level. A Canon EF 8-15 mm f/4 USM fisheye lens was used to capture the scenes. Eleven LDR images with varying exposure values (-5 t0 $+5$ with increments of $+1$) were taken for each HDR image. The circular images were fused into a single HDR photograph using Photosphere [19], [69], [76], [85], [86]. When capturing images of daylit interior spaces, there may be a chance of luminance overflow. In these cases, camera-level vertical illuminance (E_v) was used to calibrate the images, unlike luminance calibration. The HDR images from the Photosphere were cropped to 800 × 800 pixels with an exposure set to 1. The images obtained from a full-frame camera with a 180 fisheye lens had equidistant, equal-solid or hemispherical projections. Because the Canon EF 8-15 mm f/4L USM lens uses an equal solid angle (equal area) projection, the images were cosine-corrected before illuminance calibration. The calibrated HDR images with Evalglare software were used to estimate the DGP [68], [69], [76], [86]. A Konica Minolta chromameter (CL-200A) was used to measure the vertical illuminance. The complete calibration procedure and workflow have been mentioned in author's previous works, which are already mentioned in the manuscript [74], [75], [76].

Fig.10 shows sample images of glare evaluation using HDR photography and Evalglare [74]. Images were captured in previous experiments by the author at different times. For the simple evaluation of DGP with only E_v, a standard linear regression equation (Equation (5)) was found for a set of test data, which was similar to Equation (3). Equation (4) shows the linear polynomial model for the set of observations.

$$f(x) = (p1 \times x) + p2 \tag{4}$$

$$DGP = 0.185 + \left(6.998 \times 10^{-5} E_v\right) \tag{5}$$

Table 2 shows the estimated coefficients of the linear model and its goodness-of-fit. Table 3 lists the limits of the DGP for glare sensation [87], [88]. For a glare-free space, the DGP is recommended to be less than 0.3, which is imperceptible. These limits help divide the eye illuminance to avoid glare issues in a daylit space.

TABLE 2. Estimated coefficients and the goodness of fit.

Coefficients (with 95% confidence bounds)	
p1	6.998e-05 (6.904e-05, 7.093e-05)
p2	0.1851 (0.1847, 0.1855)
Goodness-of-fit	
SSE	0.002902
R-square	0.9992
Adj. R-square	0.9992
RMSE	0.002735

The preliminary visual comfort threshold for E_v is 875-1250 lux, [89] where $E_v > 1250$ lx indicates a discomfort condition. Later the same dataset was reanalyzed in another study, and a threshold value of $E_v > 1500$ lx was found. In another study, a slightly higher threshold value

FIGURE 10. HDR images and EVALGLARE results for sample images.

TABLE 3. Limits of DGP for glare sensation.

Glare sensation	DGP
Imperceptible	<0.3
Perceptible	0.30-0.35
Disturbing	0.35-0.45
Intolerable	≥0.45

of E_v as 1700 lx was found for omitting glare sensations in office environments [90]. Based on the field study carried out in two side-lit office spaces under various sky conditions, researchers [91]identified the following E_v thresholds: $E_v < 2000$ lx for 'imperceptible' glare, 2000–3000 lx for 'perceptible' glare, 3000–5000 lx for 'disturbing glare, and $E_v > 5000$ lx for 'intolerable' glare.

Similarly, [88] a threshold value of 2760 lx for the total vertical illuminance and 1000 lx for the direct vertical illuminance were proposed. In another study [92], the authors investigated glare from windows by using an epidemiological approach. This was used to test the diagnostic accuracy of different glare indices by crossing measurements, and subjective judgments in three different daylit experimental scenarios, defined as 'low', 'medium', and 'high probabilities of being disturbed by the glare source. For each scenario, a corresponding E_v thresholds of : 2600 lx, 3040 lx, and 6700 lx, respectively were identified.

Fig.11 shows the measured E_v and corresponding DGP values obtained in the test room using Evalglare. HDR images were acquired from previous experiments conducted by the author in the test room. Fig. 11 shows that an E_v of less than 1500 lx provides imperceptible glare. Hence, with the previous literature and the observations made from the test room, E_v ranges from 500 lx-1250 lx can be made available to obtain circadian entrainment. Recent studies have shown that a shorter wavelength may lead to glare issues [83]. When the blue light is greater in the morning, the maximum limit of the vertical illuminance can be fixed at lesser than 1250 lx. Because the contrast term corresponding to the luminance

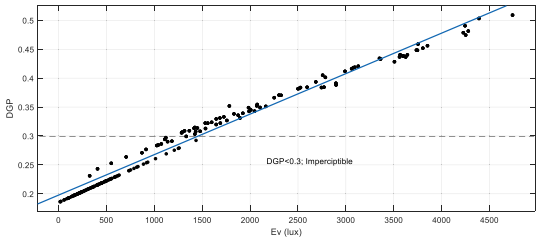

FIGURE 11. Variation in DGP with E_v.

source is not considered, this model is not applicable in cases where the sun is present a visual scene. Hence, this equation is suitable mainly for automatic shading control schemes that consider the sun position.

D. NONLINEAR REGRESSION MODEL FOR ESTIMATING CS

Nonlinear regression analysis has been widely adapted to model a function that describes the set of observations. The functions are nonlinear combinations of parameters and independent variables. Successive approximations were performed at each iteration to fit the data. The confidence interval of the estimate can be used to assess the statistical significance of a parameter. If the null value is excluded, it can be said that the parameter is statistically significant.

Here, the aim is to estimate the point-by-point CS using easily measurable photometric quantities. Hence, this model was further implemented to optimize circadian effectiveness in day-lit space. The actual equation of the CS equation is in terms of CL_A, hence it was replaced with E_v and CCT. Both quantities are strongly related to CS and are easily measurable using affordable sensors. Consequently, E_v and CCT were selected as independent parameters for the model, and the fitting function based on the actual equation of CS is proposed as follows.

$$CS\,(Ev, CCT) = 0.7 - \frac{0.7}{1 + \mathrm{a} * E_v^b * (CCT/1000)^c} \quad (6)$$

In this section, the measured CCT values are converted to nominal CCT and specified according to the CCT ANSI standard, as listed in Table 4. Manufacturers usually describe the CCT range for a particular source in nominal values. According to ANSI standards, there are 10 nominal CCT, ranging from 2200 K to 6500 K. Readings outside of these limits were rounded to the nearest hundreds. Table 3 lists the nominal CCT values and their corresponding range.

All data from the experiments and the available datasheets of the different luminaires were used to establish the mathematical model of the CS. Real-time data was used to validate the estimated model. The analysis was performed using SPSS 23.0. Levenberg-Marquardt (LM) method was used to estimate the parameters [93], [94]. The number of iterations was 50, and the sum of the square convergence and parameter convergence was fixed at 1×10^{-8}. Based on the previous literature, the initial values of parameters was 0.0001 for 'a' and 1 for 'b' and 'c', respectively. The absence of a reasonable

TABLE 4. Nominal values of CCT.

CCT_{ANSI}	CCT	CCT_{ANSI}	CCT
2200 K	(2238 ± 102) K	4000 K	(3985 ± 275) K
2500 K	(2460 ± 120) K	4500 K	(4503 ± 243) K
2700 K	(2725 ± 145) K	5000 K	(5029 ± 283) K
3000 K	(3045 ± 175) K	5700 K	(5667 ± 355) K
3500 K	(3465 ± 245) K	6500 K	(6532 ± 510) K

estimate of the initial values may lead to a local minimum rather than a global minimum.

Hence, the initial guess is crucial in the LM algorithm to avoid convergence towards the local minimum. The parameters estimated from the regression analysis are shown in Table 5. All parameters were rounded to three digits and were statistically significant; the standard error was less than 0.05. All parameters were close to their initial values. As the residual plot in fig. 12 does not show a random pattern, there is more space for improving the fitness of the model. The error plot in fig.13 shows more deviation between the observed and predicted values in the range of 3500 K-5000 K compared with other CCT's.

TABLE 5. Estimated parameters for general model.

Parameter	Estimate	Std.Error	95% Confidence interval	
			Lower Bound	Upper Bound
a	2.726×10^{-6}	<0.001	1.546×10^{-6}	3.905×10^{-6}
b	1.135	0.011	1.112	1.157
c	0.719	0.024	0.672	0.766
R2	0.919			
Adj.R2	0.919			
RMSE	0.045			

In addition, there were many outliers. Therefore, the general model induces unacceptable errors.

To improve fitness, the data were categorized as 3500 K and above. Group' a', also called 'ga' denotes the dataset for CCT $\leq$ 3500 K and group 'b' called 'gb' represents dataset above CCT > 3500 K. Also, all the outliers were removed to increase the accuracy of the models. The table shows' a', 'b', 'c', R2, Adj R2 and RMSE for both models. Both 'ga' and 'gb' models improved in R-squared and RMSE as mentioned in Tables 6 and 7. The standard error of regression (S) indicates the precision of the prediction made by the nonlinear models. This depicts the average distance of the data points from the regression line. Low value of 'S' indicates the closeness of data points to the fitness line. Here the average distance from regression line is 1.8% in'ga' and 2.5% in 'gb'.

The Akaike information criterion (AIC) is another measure used to estimate the prediction error of models. AIC expresses

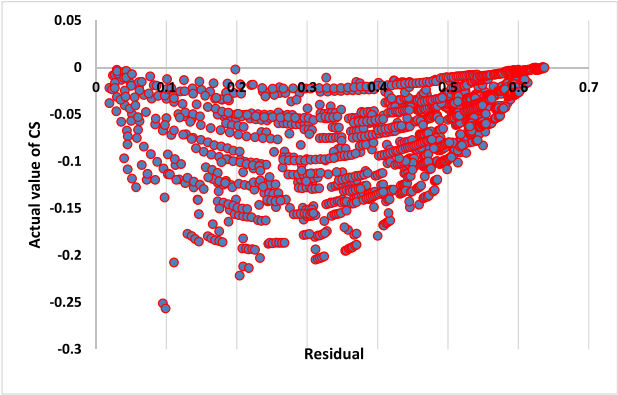

FIGURE 12. Residual plot for the predicted values of CS.

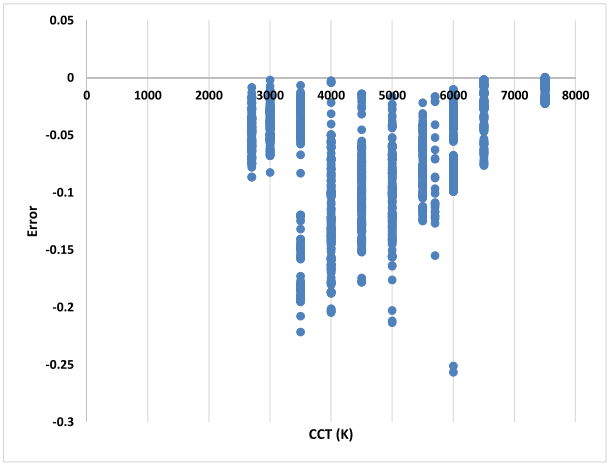

FIGURE 13. Error in predicted values of CS in various ranges of CCT.

the quality of the model by evaluating the loss of information compared to the experimental data. In other words, it is the comparison of models where the value of AIC expresses the loss of information by the model studied; the lower the value of AIC, less information loss and the more accurate and precise the model chosen.

AIC defined as follows in equation (7):

$$AIC = N * \log(\det(\frac{1}{N}\sum_{1}^{N} \varepsilon\left(t, \hat{\theta_N}\right)(\varepsilon\left(t, \hat{\theta_N}\right))^T + 2n_p + N * (n_y * (\log(2\pi) + 1)) \quad (7)$$

where,

N is the number of values in the estimation data set

$\varepsilon(t)$ is a n_y-by-1 vector of prediction errors

θ_N represents the estimated parameters

n_p is the number of estimated parameters

n_y is the number of model outputs

Model'ga' has an AIC score of −0.0024 and 'gb' −0.0045. Thus, the precision of both the models was within an acceptable range. The residual plot in fig. 14,shows more randomness compared with the residual plot in the previous general modeling.

TABLE 6. Estimated parameters for group 'ga'.

For CCT ≤ 3500 K, group 'a' ('ga')				
Parameter	Estimate	Std. Error	95% Confidence interval	
			Lower Bound	Upper Bound
a	0.001	<0.001	0.001	0.001
b	1.067	0.009	1.049	1.085
c	0.703	0.081	0.544	0.863
R2	0.983			
Adj.R2	0.983			
RMSE	0.032			
S	0.018			
AIC	-0.0024			

TABLE 7. Estimated parameters for group' gb'.

For CCT > 3500 K, group 'b' ('gb')				
Parameter	Estimate	Std. Error	95% Confidence interval	
			Lower Bound	Upper Bound
a	5.222×10^{-5}	<0.001	4.449×10^{-5}	5.995×10^{-5}
b	1.137	0.008	1.121	1.152
c	1.870	0.028	1.814	1.925
R2	0.974			
Adj.R2	0.974			
RMSE	0.032			
S	0.025			
AIC	-0.0045			

A real-time dataset was obtained for a single day from the test room to validate the above models. The data were collected from morning 10.00 am to evening 5.00 pm in 30 min.

The window on the eastside was kept open, and the measurements were taken from all occupant positions facing the computer screen. The luminaires were maintained on for the entire duration of the measurement and were not dimmed. Venetian blinds were kept 100% open for maximum daylight entry.

As in fig.15 and 16, both plots come up with accepted R^2 of 0.9972 and 0.9824 for both groups' ga' and 'gb'. All outliers were removed. These plots show the accuracies of the estimated models. These models can be further implemented to simultaneously optimize the glare and circadian effectiveness in the test room under consideration.

E. OPTIMIZATION OF DGP AND CS

Optimization techniques help develop conditional solutions for various engineering and non-engineering problems. Enhancing the test room control algorithm prioritizing circadian impact requires further understanding of the relationships between photometric variables and circadian metrics.

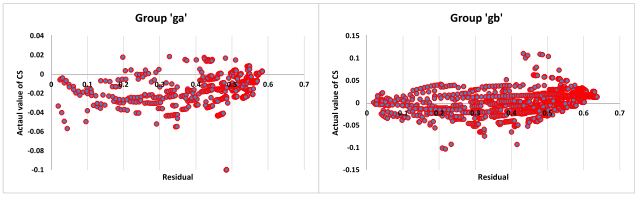

FIGURE 14. Residual plots for groups' ga' and 'gb'.

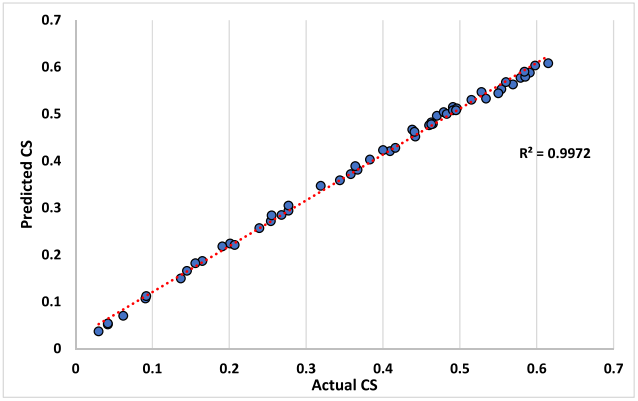

FIGURE 15. Actual CS Vs Predicted CS in 'ga'.

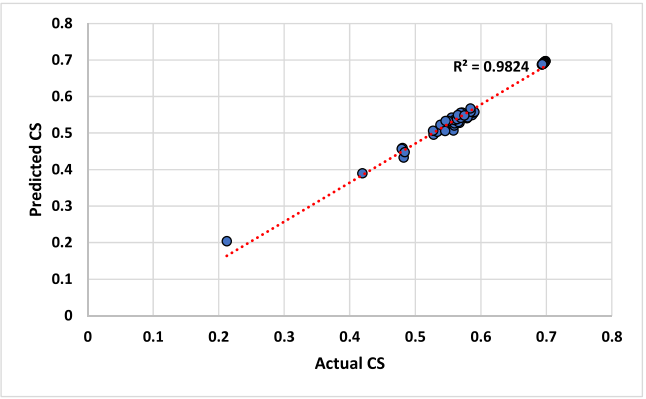

FIGURE 16. Actual CS Vs Predicted CS in 'gb'.

These relationships help incorporate circadian tunability in the present algorithm using various optimization methods. The formulation of fitness functions and their constraints is a key element in developing an optimization problem. In this study, the primary considerations for the optimization were (1) minimizing the glare and (2) maximizing the CS.

The optimized E_v and CCT were determined using the derived models for the glare and CS functions. An evolutionary optimization algorithm called Multi-Objective Genetic Algorithms (MOGA) was used to solve this problem. Simulations were performed using the GA toolbox in MATLAB. These algorithms are initialized using a randomly generated population of solutions, known as chromosomes. Each chromosome underwent a fitness evaluation using the objective functions. Chromosomes with higher fitness function values (maximizing conditions) were selected for mating in the next

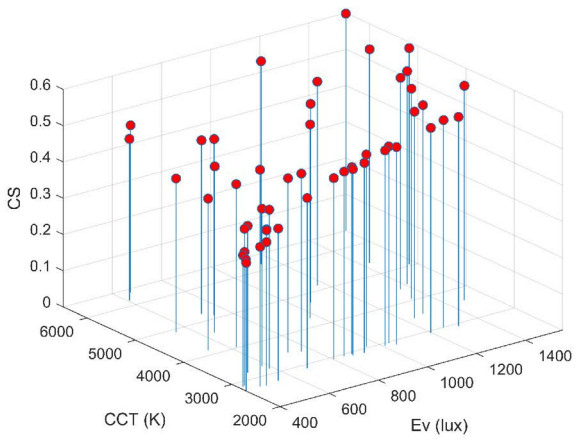

FIGURE 17. Optimum solution set of E_v and CCT.

stage. Successful chromosomes undergo crossover and generate the next generation of solutions. Random mutations were introduced to prevent convergence to a local optimum. After several iterations, as the generation progresses, the solution converges towards chromosomes with higher fitness values.

The optimization was performed under inequality constraints for minimum glare and maximum circadian stimulation within the saturation limits. DGP is restricted to <0.3 to match the typical values for glare sensation. To ensure circadian stimulation, CS was bound within 0.3 and 0.7.

This optimization aims to minimize the glare and maximize the circadian stimulation in the test workbench. The objective functions were as follows:

$$\boldsymbol{f_1(x) = DGP, f_k(x) = -CS(E_v, CCT)} \tag{8}$$

Subjected to constraints

$$\boldsymbol{f_1(x) < 0.3, \quad 0.3 \leq f_k(x) \leq 0.7} \tag{9}$$

Where k depends on the CCT range selected. ' k' is 2 for CCT greater than 3500 K lx and 3 for lesser values.
where x is the input vector which is expressed as follows

$$\mathrm{x} = \{\mathrm{E_v}, \mathrm{CCT}\}$$

Once the optimization is terminated, all solution sest that satisfy the fitness functions are considered, and invalid solutions are rejected. The pseudocode for the optimization is as follows:

Step 1: *Establish fitness functions for CS* $\boldsymbol{f_k(x)}$ *and Glare* $\boldsymbol{f_1(x)}$.
Step 2: *Set the bounds for* E_v *and CCT:* E_v *is {50, 2000}; CCT {2700, 3500} and {4000,7500}*
Step 3: *Set the constraints* $\boldsymbol{f_1(x) < 0.3, \quad 0.3 \leq f_k(x) \leq 0.7}$ *and parameters.*
Step 4: *Initialize the population size.*
Step 5: *Create random individuals.*
Step 6: *While iteration is not terminated*
Evaluate the fitness of each individual.
Selection of individuals based on fitness
Crossover and mutation are performed to change individuals.
Changse individuals in the population.
Iteration =iteration+1.
End while
Step 7: *Return the best individual* (E_v, *CCT) during evolution.*

Fig. 17 shows the optimized solution set for the minimum glare and maximum circadian triggers in the test room. All the solution set satisfy a minimum CS value of 0.3 and DGP < 0.3.

IV. DISCUSSIONS

The main objective of this study was to develop an optimization methodology for visual comfort with circadian entrainment of occupant. This optimization procedure enables the user to incorporate circadian entrainment along with visual comfort. Inaddition, this paper illustrates the impact of window orientation, the occupant's seating position, and various lighting schemes on circadian Stimuli. It helps lighting designers perform a preoccupancy evaluation of circadian effectiveness at different positions in an interior space. The suitability of the different lighting schemes in the test room was evaluated based on E_v, E_v/E_h, CS and CCT. In the DALIS mode, except for the occupant sitting on the east side where the window is kept open, all other sides are suitable for dimming settings to obtain a minimum CS value of 0.3. Circadian potential is higher when a person faces a window. However, this position is not usually preferred by the occupant because of the high possibility of glare. For an ample office space, the room's depth from the window also influences the occupant's light quantity at the eye level. Hence a person's circadian effectiveness is also affected unless there is an auxiliary light source. Although there is a uniform illuminance in the workspace, the required amount of E_v is not available at some times. Replacing a dimmable luminaire with a tunable luminaire or auxiliary light in the workspace may also provide required CS at the eye level.

Simplified mathematical models were developed to predict CS and DGP in a daylit interior space. The predictors for CS were E_v and CCT (ANSI Standards), which are easily measurable by colour and illuminance sensors and the need for expensive spectrophotometers can be discarded with this methodology. The dataset was categorized based on its nominal CCT (nominal CCT > 3500 K and nominal CCT ≤ 3500 K). While estimating the nonlinear regression models for CS, the error greater for CCT 3500 K, 4000 K and 4500 K. The individual deviation from the observed value was less in the other CCT's. These models can be improved further by adding more spectral sources to these ranges.

According to the literature and correlation test, CS is highly related to vertical eye illuminance. The CS mainly changes owing to variations in E_v. By following the changes in E_v, CS can be predicted accurately. The vertical eye illuminance (E_v) or the light level reaching the human eye varies with changes in building geometries such as room depth, ceiling

and wall reflectance factors, window size, shading elements, light sources, daylight and electric light and other external conditions such as sky type and seasonal variation. Ina ddition, as the distance from the windows changed, E_v, duv (delta uv) and CCT varied. Unless the interior space does not have uniform lighting or a controlled daylight-artificial light climate-responsive system, there are variations in the above three photometric quantities at different locations. Consequently, in these scenarios, CS also changes. Typically, CCT is used to extract the chromaticity information of general-purpose luminaires. Duv is another quantity which describes the colour quality of the light sources and ndicates the position of chromaticity with respect to the Planckian locus [95]. Duv is generally used to optimise luminaire spectra. Because, the experiment is carried out in daylit spaces and under white light sources, duv will not be more than 0.005. It can be evaluated with the knowledge of CCT and 'x','y' or 'u','v' coordinates. The deviation in duv is directly related to the CCT variation. The Prediction of CS based on CCT and duv will result in an erroneous output, because both are highly correlated. In this study, the change in climatic conditions or locations does not affect the prediction of CS since it is entirely dependent on E_v and CCT (duv). Thus if there are any changes in the climatic conditions or other factors as previously mentioned, the change in CS can be well predicted.

The lighting standards already recommend the desired horizontal illuminance (E_h) in an interior office space. It is also necessary to confirm the interior space is a glare-free lit area. For a daylit space, the commonly used glare metric is DGP (Daylight Glare Probability). A linear regression model was established for the DGP in E_v using the measured values in line with previous research. The maximum limit of vertical illuminance to reduce glare was 1500 lx. From the literature and observations, this value can be fixed at less than 1250 lux.

Ths study has some limitations. Our results do not consider the human factors such as the photic history or past exposure to light of the occupants in the room. Exposure to high levels of CS in late evenings may affect the behaviour of occupants the next morning. Hence, in reality, the behavioural patterns of occupants are important when designing an effective circadian lighting system. In addition, E_v measured at the eye level helps to predict CS. However, in an actual scenario, light reaching at the retina will be less or it is dependent on the facial contours and features of the occupants, which leads to the natural shading of the eye. Thus, the simulated CS level can be higher than the actual levels, and hence, the lighting design can achieve a minimum of CS 0.4.

Finally, both models were incorporated to minimize the glare and maximize the CS in the workspace. The MOGA has been implemented to optimize visual comfort and circadian effectiveness. This novel methodology of optimizing visual comfort and circadian effectiveness with a common predictor variable (E_v) can be easily incorporated into the daylight-artificial light integration. It is our hope that, lighting designers can effectively use these ideas for building automation that promotes circadian entrainment along with visual comfort. An additional cost of a few light sensors and colour sensors helps bring a 'healthy lighting' ambience in the interior space.

V. CONCLUSION

This study illustrates the impact of window orientation, the occupant's seating position, and various lighting schemes on circadian Stimuli. Regression models for DGP and CS were developed to remove barriers to incorporating the circadian entrainment in the automation algorithm for visual comfort. Based on the experiments and data analysis, we conclude that,

- For a daylit-office space, it is necessary to choose a proper E_v/E_h ratio to obtain CS as 0.3 and meet E_h in range of 300 lx to 500 lx, as per the IESNA standards. E_v of 500 lx provided a CS of 0.3.
- The occupant's seating position inside the daylit space plays a vital role in circadian stimulation. Even though a high E_v boosts the CS, it leads to visual discomfort to the occupants. E_v should be less than 1500 lx, so that there is no glare sensation for the occupant.
- The developed linear regression model for the DGP in E_v using the measured values aligns with previous research. Thus, the maximum limit of E_v for reducing glare was 1500 lx. During the morning, the blue light content higher and the maximum limit of vertical illuminance can be fixed at less than 1250 lx to avoid glare issues (in line with literature and observations).
- Although there is uniform illuminance in the workspace, the required amount of E_v is not available at some time. Replacing a dimmable luminaire with a tunable luminaire auxiliary light in the workspace may also provide the required CS at the eye level.
- The developed nonlinear CS estimation models have R-squared values of 0.983 and 0.974, respectively. The precision of the models was evaluated in terms of standard error of regression (S) and AIC score. S comes with a value of 1.8% and 2.5% for the models 'ga' and 'gb' respectively. −0.0024 and -0.0045 were the AIC score for models 'ga' and 'gb' respectively. This model can be implemented in the daylight-artificial light control algorithm to optimise occupants' visual comfort and circadian stimulation.
- The derived models for CS and DGP were used to optimize glare and circadian stimulation. Using GA, the multi-objective optimization evaluated the minimum values of CCT and E_v to obtain glare-free light and circadian boosting.
- Optimizing daylight-artificial light scheme with climate-responsive automated shading control and Luminaire dimming taking CS also as a variant in addition to visual comfort, thermal comfort and energy efficiency is the future requirement.

DECLARATION OF CONFLICTING INTERESTS

The authors declare no potential conflicts of interest concerning the research, authorship, and publication of this manusript.

ACKNOWLEDGMENT

The authors would like to thank PG students Kanniha and Pavithra for their help in data collection and the Technicians of Lighting Measurements Laboratory, Manipal Institute of Technology (MIT), Manipal, for their support in the experiment.

REFERENCES

[1] M. Hastings, J. S. O'Neill, and E. S. Maywood, "Circadian clocks: Regulators of endocrine and metabolic rhythms," *J. Endocrinol.*, vol. 195, pp. 187–198, Nov. 2007, doi: 10.1677/JOE-07-0378.

[2] P. Boyce, "Editorial: Exploring human-centric lighting," *Lighting Res. Technol.*, vol. 48, no. 2, p. 101, 2016, doi: 10.1177/1477153516634570.

[3] K. P. Wright, A. W. McHill, B. R. Birks, B. R. Griffin, T. Rusterholz, and E. D. Chinoy, "Entrainment of the human circadian clock to the natural light-dark cycle," *Current Biol.*, vol. 23, no. 16, pp. 1554–1558, Aug. 2013, doi: 10.1016/j.cub.2013.06.039.

[4] M. Rea, M. Figueiro, A. Bierman, and R. Hamner, "Modelling the spectral sensitivity of the human circadian system," *Lighting Res. Technol.*, vol. 44, no. 4, pp. 386–396, Dec. 2012, doi: 10.1177/1477153511430474.

[5] R. J. Lucas, "Measuring and using light in the melanopsin age," *Trends Neurosci.*, vol. 37, pp. 1–9, Jan. 2014, doi: 10.1016/j.tins.2013.10.004.

[6] M. S. Rea, M. G. Figueiro, J. D. Bullough, and A. Bierman, "A model of phototransduction by the human circadian system," *Brain Res. Rev.*, vol. 50, no. 2, pp. 213–228, Dec. 2005, doi: 10.1016/j.brainresrev.2005.07.002.

[7] A. J. Lewy, T. A. Wehr, F. K. Goodwin, D. A. Newsome, and S. P. Markey, "Light suppresses melatonin secretion in humans," *Science*, vol. 210, no. 4475, pp. 1267–1269, Dec. 1980, doi: 10.1126/science.7434030.

[8] G. C. Brainard, J. P. Hanifin, and J. M. Greeson, "Action spectrum for melatonin regulation in humans: Evidence for a novel circadian photoreceptor," *J. Neurosci.*, vol. 21, no. 16, pp. 6405–6412, 2001, doi: 10.1523/jneurosci.21-16-06405.2001.

[9] M. Boubekri, I. N. Cheung, K. J. Reid, C.-H. Wang, and P. C. Zee, "Impact of Windows and daylight exposure on overall health and sleep quality of office workers: A case-control pilot study," *J. Clin. Sleep Med.*, vol. 10, no. 6, pp. 603–611, Jun. 2014, doi: 10.5664/jcsm.3780.

[10] Y. de Kort and K. Smolders, "Effects of dynamic lighting on office workers: First results of a field study with monthly alternating settings," *Lighting Res. Technol.*, vol. 42, no. 3, pp. 345–360, Sep. 2010, doi: 10.1177/1477153510378150.

[11] M. Rea and M. Figueiro, "Light as a circadian stimulus for architectural lighting," *Lighting Res. Technol.*, vol. 50, no. 4, pp. 497–510, Jun. 2018, doi: 10.1177/1477153516682368.

[12] M. Figueiro, R. Nagare, and L. Price, "Non-visual effects of light: How to use light to promote circadian entrainment and elicit alertness," *Lighting Res. Technol.*, vol. 50, no. 1, pp. 38–62, Jan. 2018, doi: 10.1177/1477153517721598.

[13] M. G. Figueiro, B. Steverson, J. Heerwagen, K. Kampschroer, C. M. Hunter, K. Gonzales, B. Plitnick, and M. S. Rea, "The impact of daytime light exposures on sleep and mood in office workers," *Sleep Health*, vol. 3, no. 3, pp. 204–215, Jun. 2017, doi: 10.1016/j.sleh.2017.03.005.

[14] T. W. Kim, J.-H. Jeong, and S.-C. Hong, "The impact of sleep and circadian disturbance on hormones and metabolism," *Int. J. Endocrinol.*, vol. 2015, pp. 1–9, Jan. 2015, doi: 10.1155/2015/591729.

[15] J. van Duijnhoven, M. P. J. Aarts, M. B. C. Aries, A. L. P. Rosemann, and H. S. M. Kort, "Systematic review on the interaction between office light conditions and occupational health: Elucidating gaps and methodological issues," *Indoor Built Environ.*, vol. 28, no. 2, pp. 152–174, Feb. 2019, doi: 10.1177/1420326X17735162.

[16] K. Thapan, J. Arendt, and D. J. Skene, "An action spectrum for melatonin suppression: Evidence for a novel non-rod, non-cone photoreceptor system in humans," *J. Physiol.*, vol. 535, pp. 261–267, Aug. 2001.

[17] S. Berman and R. Clear, "A practical metric for melanopic metrology," *Lighting Res. Technol.*, vol. 51, no. 8, pp. 1178–1191, Dec. 2019, doi: 10.1177/1477153518824147.

[18] J. A. Enezi, V. Revell, T. Brown, J. Wynne, L. Schlangen, and R. Lucas, "A 'melanopic' spectral efficiency function predicts the sensitivity of melanopsin photoreceptors to polychromatic lights," *J. Biol. Rhythms*, vol. 26, no. 4, pp. 314–323, Aug. 2011, doi: 10.1177/0748730411409719.

[19] B. Jung and M. Inanici, "Measuring circadian lighting through high dynamic range photography," *Lighting Res. Technol.*, vol. 51, no. 5, pp. 742–763, Aug. 2018, doi: 10.1177/1477153518792597.

[20] Z. Richardson, "The WELL building standard: Assessment of effectiveness," Bachelor's Thesis, California Polytech. State Univ., San Luis Obispo, CA, USA, 2018. [Online]. Available: https://digitalcommons.calpoly.edu/cmsp/127

[21] *DIN SPEC 5031-100 Optical Radiation Physics and Illuminating Engineering—Part 100: Melanopic Effects of Ocular Light on Human Beings—Quantities, Symbols and Action Spectra*, Deutsches Institut Normung, Berlin, Germany, 2015.

[22] *DIN SPEC 67600 Biologically Effective Illumination—Design Guidelines*, Deutsches Institut Normung, Berlin, Germany, 2013.

[23] *Commission Internationale de l'Eclairage CIE S 026/E: 2018 CIE System for Metrology of Optical Radiation for ipRGC-Influenced Responses to Light*, CIE, Vienna, Austria, 2018.

[24] M. G. Figueiro, K. Gonzales, and D. Pedler. *Circadian Stimulus the Lighting Research Center Proposes a Metric for Applying Circadian Light in the Built Environment*. Accessed: Oct. 31, 2016. [Online]. Available: https://www.ies.org

[25] M. S. Rea, M. G. Figueiro, A. Bierman, and J. D. Bullough, "Circadian light," *J. Circadian Rhythms*, vol. 8, p. 2, Feb. 2010, doi: 10.1186/1740-3391-8-2.

[26] M. Figueiro and M. Rea, "Office lighting and personal light exposures in two seasons: Impact on sleep and mood," *Lighting Res. Technol.*, vol. 48, no. 3, pp. 352–364, May 2016, doi: 10.1177/1477153514564098.

[27] M. S. Rea, M. G. Figueiro, A. Bierman, and J. D. Bullough, "Circadian light," *J. Circadian Rhythms*, vol. 8, p. 2, Feb. 2010, doi: 10.1186/1740-3391-8-2.

[28] I. Acosta, M. Á. Campano, R. Leslie, and L. Radetsky, "Daylighting design for healthy environments: Analysis of educational spaces for optimal circadian stimulus," *Sol. Energy*, vol. 193, pp. 584–596, Nov. 2019, doi: 10.1016/j.solener.2019.10.004.

[29] M. Andersen, S. J. Gochenour, and S. W. Lockley, "Modelling 'non-visual' effects of daylighting in a residential environment," *Building Environ.*, vol. 30, pp. 138–149, Dec. 2013, doi: 10.1016/j.buildenv.2013.08.018.

[30] K. Konis, "A novel circadian daylight metric for building design and evaluation," *Building Environ.*, vol. 113, pp. 22–38, Feb. 2017, doi: 10.1016/j.buildenv.2016.11.025.

[31] Y. Zhu, M. Yang, Y. Yao, X. Xiong, X. Li, G. Zhou, and N. Ma, "Effects of illuminance and correlated color temperature on daytime cognitive performance, subjective mood, and alertness in healthy adults," *Environ. Behav.*, vol. 51, no. 2, pp. 199–230, Feb. 2019, doi: 10.1177/0013916517738077.

[32] P. Bodrogi, Q. Vinh, and T. Khanh, "Correlations among lighting quality metrics for interior lighting," *Lighting Res. Technol.*, vol. 51, no. 8, pp. 1192–1207, Dec. 2019, doi: 10.1177/1477153518818856.

[33] Q. Dai, W. Cai, W. Shi, L. Hao, and M. Wei, "A proposed lighting-design space: Circadian effect versus visual illuminance," *Building Environ.*, vol. 122, pp. 287–293, Sep. 2017, doi: 10.1016/j.buildenv.2017.06.025.

[34] Q. Yao, W. Cai, M. Li, Z. Hu, P. Xue, and Q. Dai, "Efficient circadian daylighting: A proposed equation, experimental validation, and the consequent importance of room surface reflectance," *Energy Buildings*, vol. 210, Mar. 2020, Art. no. 109784, doi: 10.1016/j.enbuild.2020.109784.

[35] W. Cai, J. Yue, Q. Dai, L. Hao, Y. Lin, W. Shi, Y. Huang, and M. Wei, "The impact of room surface reflectance on corneal illuminance and rule-of-thumb equations for circadian lighting design," *Building Environ.*, vol. 141, pp. 288–297, Aug. 2018, doi: 10.1016/j.buildenv.2018.05.056.

[36] Q. Dai, Y. Huang, L. Hao, Y. Lin, and K. Chen, "Spatial and spectral illumination design for energy-efficient circadian lighting," *Building Environ.*, vol. 146, pp. 216–225, Dec. 2018, doi: 10.1016/j.buildenv.2018.10.004.

[37] L. Bellia, F. Bisegna, and G. Spada, "Lighting in indoor environments: Visual and non-visual effects of light sources with different spectral power distributions," *Building Environ.*, vol. 46, no. 10, pp. 1984–1992, Dec. 2011, doi: 10.1016/j.buildenv.2011.04.007.

[38] T. Ru, Y. A. W. de Kort, K. C. H. J. Smolders, Q. Chen, and G. Zhou, "Non-image forming effects of illuminance and correlated color temperature of office light on alertness, mood, and performance across cognitive domains," *Building Environ.*, vol. 149, pp. 253–263, Feb. 2019, doi: 10.1016/j.buildenv.2018.12.002.

[39] B. Fabio, B. Chiara, L. R. Ornella, B. Laura, and F. Simonetta, "Non-visual effects of light: An overview and an Italian experience," *Energy Proc.*, vol. 78, pp. 723–728, Nov. 2015, doi: 10.1016/j.egypro.2015.11.080.

[40] J. Nie, T. Zhou, Z. Chen, W. Dang, F. Jiao, J. Zhan, Y. Chen, Y. Chen, Z. Pan, X. Kang, Y. Wang, Q. Wang, W. Dong, S. Zhou, X. Yu, G. Zhang, and B. Shen, "Investigation on entraining and enhancing human circadian rhythm in closed environments using daylight-like LED mixed lighting," *Sci. Total Environ.*, vol. 732, Aug. 2020, Art. no. 139334, doi: 10.1016/j.scitotenv.2020.139334.

[41] J. Nawyn, M. Thompson, N. Chen, and K. Larson, "A closed-loop feedback system for a context-aware tunable architectural lighting application," *Hum. Factors Ergonom. Soc. Annu. Meeting*, vol. 56, no. 1, pp. 541–545, Sep. 2012, doi: 10.1177/1071181312561113.

[42] W. Hertog, A. Llenas, J. M. Quintero, C. E. Hunt, and J. Carreras, "Energy efficiency and color quality limits in artificial light sources emulating natural illumination," *Opt. Exp.*, vol. 22, no. S7, p. A1659, Dec. 2014, doi: 10.1364/oe.22.0a1659.

[43] E. V. Ellis, E. W. Gonzalez, D. A. Kratzer, D. L. McEachron, and G. Yeutter, "Auto-tuning daylight with LEDs: Sustainable lighting for health and well-being," in *Proc. ARCC Spring Res. Conf.*, 2013, pp. 465–473. [Online]. Available: http://www.arcc-journal.org/index.php/repository/article/view/202

[44] W. Hertog, A. Llenas, and J. Carreras, "Optimizing indoor illumination quality and energy efficiency using a spectrally tunable lighting system to augment natural daylight," *Opt. Exp.*, vol. 23, no. 24, p. A1564, Nov. 2015, doi: 10.1364/oe.23.0a1564.

[45] R. G. Hopkinson, "Glare from daylighting in buildings," *Appl. Ergonom.*, vol. 3, no. 4, pp. 206–215, 1972, doi: 10.1016/0003-6870(72)90102-0.

[46] P. Petherbridge and R. G. Hopkinson, "Discomfort glare and the lighting of buildings," *Lighting Res. Technol.*, vol. 15, no. 2, pp. 39–79, Feb. 1950, doi: 10.1177/147715355001500201.

[47] C. Pierson, J. Wienold, and M. Bodart, "Discomfort glare perception in daylighting: Influencing factors," *Energy Proc.*, vol. 122, pp. 331–336, Sep. 2017, doi: 10.1016/j.egypro.2017.07.332.

[48] Y. Bian, T. Leng, and Y. Ma, "A proposed discomfort glare evaluation method based on the concept of 'adaptive zone,'" *Building Environ.*, vol. 143, pp. 306–317, Oct. 2018, doi: 10.1016/j.buildenv.2018.07.025.

[49] T. Iwata and M. Tokura, "Position index for a glare source located below the line of vision," *Lighting Res. Technol.*, vol. 29, no. 3, pp. 172–178, Sep. 1997, doi: 10.1177/14771535970290030801.

[50] S. Torres and V. R. M. L. Verso, "Comparative analysis of simplified daylight glare methods and proposal of a new method based on the cylindrical illuminance," *Energy Proc.*, vol. 78, pp. 699–704, Nov. 2015, doi: 10.1016/j.egypro.2015.11.074.

[51] S. G. Varghese, C. P. Kurian, V. I. George, M. Varghese, and T. M. Sanjeev Kumar, "Climate model-based test workbench for daylight-artificial light integration," *Lighting Res. Technol.*, vol. 4, pp. 1–14, Oct. 2018, doi: 10.1177/1477153518792586.

[52] S. G. Varghese, C. P. Kurian, V. I. George, and T. S. S. Kumar, "Daylight-artificial light integrated scheme based on digital camera and wireless networked sensing-actuation system," *IEEE Trans. Consum. Electron.*, vol. 65, no. 3, pp. 284–292, Aug. 2019, doi: 10.1109/TCE.2019.2924078.

[53] C. Kurian, R. Aithal, J. Bhat, and V. George, "Robust control and optimisation of energy consumption in daylight—Artificial light integrated schemes," *Lighting Res. Technol.*, vol. 40, no. 1, pp. 7–24, Mar. 2008, doi: 10.1177/1477153507079511.

[54] D. Kolokotsa, D. Tsiavos, G. S. Stavrakakis, K. Kalaitzakis, and E. Antonidakis, "Advanced fuzzy logic controllers design and evaluation for buildings' occupants thermal–visual comfort and indoor air quality satisfaction," *Energy Buildings*, vol. 33, no. 6, pp. 531–543, 2001, doi: 10.1016/S0378-7788(00)00098-0.

[55] J. M. Dussault and L. Gosselin, "Office buildings with electrochromic windows: A sensitivity analysis of design parameters on energy performance, and thermal and visual comfort," *Energy Buildings*, vol. 153, pp. 50–62, Oct. 2017, doi: 10.1016/j.enbuild.2017.07.046.

[56] L. Sanati and M. Utzinger, "The effect of window shading design on occupant use of blinds and electric lighting," *Building Environ.*, vol. 64, pp. 67–76, Jun. 2013, doi: 10.1016/j.buildenv.2013.02.013.

[57] S. Firlág, M. Yazdanian, C. Curcija, C. Kohler, S. Vidanovic, R. Hart, and S. Czarnecki, "Control algorithms for dynamic Windows for residential buildings," *Energy Buildings*, vol. 109, pp. 157–173, Dec. 2015, doi: 10.1016/j.enbuild.2015.09.069.

[58] F. Gugliermetti and F. Bisegna, "Visual and energy management of electrochromic windows in Mediterranean climate," *Building Environ.*, vol. 38, no. 3, pp. 479–492, 2003, doi: 10.1016/S0360-1323(02)00124-5.

[59] W. J. Hee, M. A. Alghoul, and B. Bakhtyar, "The role of window glazing on daylighting and energy saving in buildings," *Renew. Sustain. Energy Rev.*, vol. 42, pp. 323–343, Feb. 2015, doi: 10.1016/j.rser.2014.09.020.

[60] S. Jain and V. Garg, "A review of open loop control strategies for shades, blinds and integrated lighting by use of real-time daylight prediction methods," *Building Environ.*, vol. 135, pp. 352–364, Dec. 2018, doi: 10.1016/j.buildenv.2018.03.018.

[61] N. Aste, J. Compostella, and M. Mazzon, "Comparative energy and economic performance analysis of an electrochromic window and automated external venetian blind," *Energy Proc.*, vol. 30, no. Feb. 2014, pp. 404–413, 2012, doi: 10.1016/j.egypro.2012.11.048.

[62] M. Bauer, J. Geiginger, W. Hegetschweiler, G. Sejkora, N. Morel, P. Wurmsdobler, "DELTA, a blind controller using fuzzy logic," Final OFEN Rep., LESO-PB, EPFL, Lausanne, Switzerland, 1996.

[63] N. Morel, M. Bauer, M. El-Khoury, and J. Krauss, "Neurobat, a predictive and adaptive heating control system using artificial neural networks," *Int. J. Solar Energy*, vol. 21, nos. 2–3, pp. 161–201, 2001.

[64] A. Bierman, T. R. Klein, and M. S. Rea, "The Daysimeter: A device for measuring optical radiation as a stimulus for the human circadian system," *Meas. Sci. Technol.*, vol. 16, no. 11, p. 2292, 2005, doi: 10.1088/0957-0233/16/11/023.

[65] D. Pollard and P. Radchenko, "Nonlinear least-squares estimation," *J. Multivariate Anal.*, vol. 97, no. 2, pp. 548–562, Feb. 2006, doi: 10.1016/j.jmva.2005.04.002.

[66] W. Truong, V. Trinh, and T. Khanh, "Circadian stimulus—A computation model with photometric and colorimetric quantities," *Lighting Res. Technol.*, vol. 52, no. 6, pp. 751–762, Oct. 2020, doi: 10.1177/1477153519887423.

[67] K. Konis, "Predicting visual comfort in side-lit open-plan core zones: Results of a field study pairing high dynamic range images with subjective responses," *Energy Buildings*, vol. 77, 2014, doi: 10.1016/j.enbuild.2014.03.035.

[68] J. Wienold and J. Christoffersen, "Evaluation methods and development of a new glare prediction model for daylight environments with the use of CCD cameras," *Energy Buildings*, vol. 38, no. 7, pp. 743–757, Jul. 2006, doi: 10.1016/j.enbuild.2006.03.017.

[69] J. Suk and M. Schiler, "Investigation of evalglare software, daylight glare probability and high dynamic range imaging for daylight glare analysis," *Lighting Res. Technol.*, vol. 45, no. 4, pp. 450–463, Aug. 2013, doi: 10.1177/1477153512458671.

[70] J. Wienold, T. Iwata, M. Sarey Khanie, E. Erell, E. Kaftan, R. Rodriguez, J. Yamin Garreton, T. Tzempelikos, I. Konstantzos, J. Christoffersen, T. Kuhn, C. Pierson, and M. Andersen, "Cross-validation and robustness of daylight glare metrics," *Lighting Res. Technol.*, vol. 51, no. 7, pp. 983–1013, Nov. 2019, doi: 10.1177/1477153519826003.

[71] J. Wienold, "Dynamic simulation of blind control strategies for visual comfort and energy balance analysis," in *Building Simulation*. Beijing, China: IBPSA, 2007, pp. 1197–1204.

[72] Y. J. Saw, V. Kalavally, and C. P. Tan, "The spectral optimization of a commercializable multi-channel LED panel with circadian impact," *IEEE Access*, vol. 8, pp. 136498–136511, 2020, doi: 10.1109/ACCESS.2020.3010339.

[73] K. Deb, A. Pratap, S. Agarwal, and T. Meyarivan, "A fast and elitist multiobjective genetic algorithm: NSGA-II," *IEEE Trans. Evol. Comput.*, vol. 6, no. 2, pp. 182–197, Apr. 2002, doi: 10.1109/4235.996017.

[74] T. M. Sanjeev Kumar, C. P. Kurian, and S. G. Varghese, "Ensemble Learning model-based test workbench for the optimization of building energy performance and occupant comfort," *IEEE Access*, vol. 8, pp. 96075–96087, 2020, doi: 10.1109/ACCESS.2020.2996546.

[75] C. Kurian and S. Shetty, "A data-driven approach for the control of a daylight-artificial light integrated scheme," *Lighting Res. Technol.*, vol. 52, no. 2, pp. 293–313, 2019, doi: 10.1177/1477153519841104.

[76] C. P. Kurian and S. G. Varghese, "High dynamic range imaging system for energy optimization in daylight—Artificial light integrated scheme," *Int. J. Renew. Energy Res.*, vol. 5, no. 2, pp. 435–442, 2015.

[77] S. Colaco, C. Kurian, V. George, and A. Colaco, "Integrated design and real-time implementation of an adaptive, predictive light controller," *Lighting Res. Technol.*, vol. 44, no. 4, pp. 459–476, Dec. 2012, doi: 10.1177/1477153512445713.

[78] P. Chauvel, J. B. Collins, R. Dogniaux, and J. Longmore, "Glare from windows: Current views of the problem," *Lighting Res. Technol.*, vol. 14, no. 1, pp. 31–46, Mar. 1982, doi: 10.1177/096032718201400103.

[79] J.-M. Dussault, M. Sourbron, and L. Gosselin, "Reduced energy consumption and enhanced comfort with smart windows: Comparison between quasi-optimal, predictive and rule-based control strategies," *Energy Buildings*, vol. 127, pp. 680–691, Sep. 2016, doi: 10.1016/j.enbuild.2016.06.024.
[80] S. Jaber and S. Ajib, "Thermal and economic windows design for different climate zones," *Energy Buildings*, vol. 43, no. 11, pp. 3208–3215, 2011, doi: 10.1016/j.enbuild.2011.08.019.
[81] Y. Ajaji and P. André, "Thermal comfort and visual comfort in an office building equipped with smart electrochromic glazing: An experimental study," *Energy Proc.*, vol. 78, pp. 2464–2469, Nov. 2015, doi: 10.1016/j.egypro.2015.11.230.
[82] I. Acosta, R. P. Leslie, and M. G. Figueiro, "Analysis of circadian stimulus allowed by daylighting in hospital rooms," *Lighting Res. Technol.*, vol. 49, no. 1, pp. 49–61, 2017, doi: 10.1177/1477153515592948.
[83] M. Sivak, B. Schoettle, T. Minoda, and M. J. Flannagan, "Short-wavelength content of LED headlamps and discomfort glare," *LEUKOS*, vol. 2, no. 2, pp. 145–154, Oct. 2005, doi: 10.1582/LEUKOS.2005.02.02.006.
[84] *IESNA Lightning Handbook*, IESNA, New York, NY, USA, 2018.
[85] C. Pierson, C. Cauwerts, M. Bodart, and J. Wienold, "Tutorial: Luminance maps for daylighting studies from high dynamic range photography," *LEUKOS*, vol. 17, no. 2, pp. 140–169, Apr. 2021, doi: 10.1080/15502724.2019.1684319.
[86] M. Schiler and J. Y. Suk, "Response to correspondence: Investigation of evalglare software, daylight glare probability and high dynamic range imaging for daylight glare analysis," *Lighting Res. Technol.*, vol. 50, no. 2, pp. 331–332, Apr. 2018, doi: 10.1177/1477153518758614.
[87] J. Y. Suk, M. Schiler, and K. Kensek, "Investigation of existing discomfort glare indices using human subject study data," *Building Environ.*, vol. 113, pp. 121–130, Feb. 2017, doi: 10.1016/j.buildenv.2016.09.018.
[88] I. Konstantzos, A. Tzempelikos, and Y.-C. Chan, "Experimental and simulation analysis of daylight glare probability in offices with dynamic window shades," *Building Environ.*, vol. 87, pp. 244–254, May 2015, doi: 10.1016/j.buildenv.2015.02.007.
[89] K. Van Den Wymelenberg and M. Inanici, "A critical investigation of common lighting design metrics for predicting human visual comfort in offices with daylight," *LEUKOS*, vol. 10, no. 3, pp. 145–164, Jul. 2014, doi: 10.1080/15502724.2014.881720.
[90] L. Karlsen, P. Heiselberg, I. Bryn, and H. Johra, "Verification of simple illuminance based measures for indication of discomfort glare from Windows," *Building Environ.*, vol. 92, pp. 615–626, Oct. 2015, doi: 10.1016/j.buildenv.2015.05.040.
[91] Y. Bian and T. Luo, "Investigation of visual comfort metrics from subjective responses in China: A study in offices with daylight," *Building Environ.*, vol. 123, pp. 661–671, Oct. 2017, doi: 10.1016/j.buildenv.2017.07.035.
[92] R. G. Rodriguez, J. A. Yamín Garretón, and A. E. Pattini, "An epidemiological approach to daylight discomfort glare," *Building Environ.*, vol. 113, pp. 39–48, Feb. 2017, doi: 10.1016/j.buildenv.2016.09.028.
[93] A. Ranganathan. (Jun. 2004). *The Levenberg-Marquardt Algorithm*. [Online]. Available:https://excelsior.cs.ucsbeducoursescs290ipdfL.MA.pdf
[94] H. P. Gavin, "The Levenberg-Marquardt algorithm for nonlinear least squares curve-fitting problems," Dept. Civil Environ. Eng., Duke Univ., Durham, NC, USA, Aug. 2019.
[95] Y. Ohno, "Practical use and calculation of CCT and duv," *LEUKOS*, vol. 10, no. 1, pp. 47–55, Jan. 2014, doi: 10.1080/15502724.2014.839020.

VEENA MATHEW (Member, IEEE) received the B.Tech. degree in electrical and electronics engineering from the Mar Athanasius College of Engineering, India, in 2011, and the M.Tech. degree in process control and instrumentation from the National Institute of Technology, Tiruchirappalli, India, 2014. She is currently pursuing the Ph.D. degree with the Electrical and Electronics Engineering Department, Manipal Institute of Technology, Manipal Academy of Higher Education, Manipal, India.

Her research interests include sustainable building, building energy efficiency, human-centric lighting, thermal and visual comfort, control systems, optimization, and artificial intelligence.

CIJI PEARL KURIAN (Senior Member, IEEE) was born in India, in 1964. She received the B.Tech. degree in electrical and electronics engineering from Calicut University, Kerala, in 1986, the M.Tech. degree in lighting science and engineering from Mangalore University, Karnataka, in 1994, and the Ph.D. degree in electrical engineering from Manipal University, Manipal, India, in 2007.

Since 1987, she has been teaching with the Electrical and Electronics Engineering Department, Manipal Institute of Technology, Manipal, a constituent institution of the Manipal Academy of Higher Education, India. Her research interests include lighting controls-technology and applications.

Dr. Kurian is a fellow of the Institution of Engineers India and a Life Member of professional bodies, such as the Indian Society of Lighting Engineers, the Indian Society for Technical Education, and the Systems Society of India. She is an Associate Editor of the journal *Manipal Journal of Science and Technology* (MJST).

NEVIN AUGUSTINE received the B.Tech. degree in applied electronics and instrumentation from the College of Engineering, Trivandrum, India, in 2011, and the M.Tech. degree in process control and instrumentation from the National Institute of Technology, Tiruchirappalli, India, in 2014.

He is currently a Faculty and a Research Scholar at the Manipal Institute of Technology, MAHE, Manipal, India. He has seven years of teaching and industrial experience. His research interests include MEMS, vibration energy harvesting, control systems, and instrumentation system design.